

New basic insights on the potential of a chitosan-based medical device for improving functional recovery after radical prostatectomy

Luisa Muratori*, Federica Fregnan*, Giulia Ronchi*, Kirsten Haastert-Talini†, Jennifer Metzen‡, Riccardo Bertolo§, Francesco Porpiglia¶, ** and Stefano Geuna*

*Department of Clinical and Biological Sciences, Cavalieri Ottolenghi Neuroscience Institute, University of Turin, Orbassano, Italy, †Hannover Medical School, Institute of Neuroanatomy and Cell Biology, Center for Systems Neuroscience (ZSN), ‡Hannover Medical School, Institute of Neuroanatomy and Cell Biology, Hannover, Germany, §Glickman Urological and Kidney Institute, Cleveland Clinic, Cleveland, OH, USA, ¶Division of Urology, Department of Oncology, and **Department of Clinical and Biological Sciences, San Luigi Gonzaga Hospital, University of Turin, Orbassano, Italy

L.M. and F.F. contributed equally to this work

Objectives

To evaluate: (i) the neuro-regenerative potential of chitosan membrane (CS-Me) on acutely axotomised autonomic neurones *in vitro*; (ii) to exclude the possibility that a pro-regenerative biomaterial could interfere with the proliferation activity of prostate cancer cell lines; (iii) to provide an *in vivo* proof of the biocompatibility and regeneration promoting effect of CS-Me in a standardised rat model of peripheral nerve injury and repair; (iv) finally, to evaluate the tissue reaction induced by the degrading material; as previous studies have shown promising effects of CS-Me for protection of the neurovascular bundles for potency recovery in patients that undergo nerve-sparing radical prostatectomy (RP).

Materials and Methods

Addressing aim (i), the neuro-regenerative potential, organotypic cultures derived from primary sympathetic ganglia were cultured on CS-Me over 3 days and neurite extension and axonal sprouting were evaluated. Addressing aim (ii), effects of CS on cancer cells, different human prostate cancer cell lines (PC3, DU-145, LN-Cap) were seeded on CS-coated plates or cultured in the presence of CS-Me dissolution products. Addressing aims (iii) and (iv), functional recovery of peripheral nerve fibres and tissue reaction with the biomaterial, CS-Me and CS nerve guides were used to repair a median nerve injury in the rat.

Introduction

Prostate cancer is the most common cancer amongst men. An incidence of 214/1000 cases is registered in Europe, surpassing the number of the lung and colorectal cancers [1] and representing the second leading cause of cancer mortality [2].

Functional recovery was evaluated during the post-recovery time by the behavioural grasping test.

Results

CS-Me significantly stimulated axon elongation from autonomic ganglia in comparison to control conditions in organotypic three-dimensional cultures. CS coating, as well as the dissolution products of CS-Me, led to a significantly lower proliferation rate of prostate cancer cell lines *in vitro*. Tissue reaction towards CS-Me and standard CS nerve guides was similar in the rat median nerve model, as was the outcome of nerve fibre regeneration and functional recovery.

Conclusion

The results of this study provide the first experimental evidence in support of the clinical safety of CS-Me and of their postulated effectiveness for improving functional recovery after RP. The presented results are coherent in demonstrating that acutely axotomised autonomic neurones show increased neurite outgrowth on CS-Me substrate, whilst the same substrate reduces prostate cancer cell line proliferation *in vitro*. Furthermore, CS-Me do not demonstrate any disadvantage for peripheral nerve repair in a standard animal model.

Keywords

chitosan, autonomic ganglia, prostate cancer, nerve regeneration

The current most popular treatment of localised prostate cancer in patients with a life-expectancy >10 years is radical prostatectomy (RP; European Association of Urology Guidelines on Prostate Cancer, 2017 update). Unfortunately, in patients who undergo RP, frequently iatrogenic damage to the periprostatic neurovascular bundles (NVBs) occurs, leading to erectile dysfunction [3].

There has been much effort to promote a more rapid and efficient recovery of functions, namely potency and continence, after RP. Patel *et al.* [4] conducted a pivotal study aimed at determining if the use of a dehydrated human amnion/chorion membrane (dHACM) allograft wrapped around the NVBs during robot-assisted RP (RARP) is able to accelerate the return to normal functioning. Interestingly, the authors did demonstrate that the application of dHACM in patients accelerates the recovery of potency and continence, compared to patients who did not receive the membranes.

Recently, the application of membranes made of another biomaterial of natural origin, namely the chitosan membrane (CS-Me), on the NVBs after nerve-sparing RARP has been reported to be safe. The authors also reported encouraging results regarding recovery of potency [5]. This indicates that application of CS-Me after nerve-sparing RP may serve as a valuable adjunct approach to support functional recovery of the periprostatic NVB and its target tissue.

Starting from the promising clinical evidence, the studies presented in the present paper were designed to test this hypothesis and thereby provide a pre-clinical science basis for further clinical translation. As no standardised pre-clinical models exist for evaluating the effect of biomaterials to be applied after RP in men, we selected the rat median nerve model as an alternative. The rat median nerve model is a well-established and valuable model to elucidate effects of an implanted biomaterial on the regeneration of axotomised neurones towards re-innervation of peripheral target tissue [6,7].

Our present studies were specifically aimed at: (i) investigating the neuro-regenerative effect of CS-Me on *ex vivo* cultures of acutely axotomised primary autonomic ganglia; (ii) excluding a potential modifying effect on prostatic cancer cell growth following oncological surgery for cancer cells in contact with CS surfaces and CS dissolution products; (iii) conducting a morphometric analysis of regenerated nerve fibres and evaluating the functional recovery in a standardised rat preclinical model of median nerve lesion repaired with a CS-Me; (iv) finally, to evaluate the tissue reaction induced by the degrading material.

Materials and Methods

CS-Me Preparation

CS, made up of $\beta(1-4)$ linked D-glucosamine and N-acetyl-D-glucosamine subunits, is the partially or fully deacetylated form of chitin, which is found widely in nature in the exoskeletons of arthropods, shells of crustaceans. However, being a carbohydrate, persons allergic to shellfish protein, will not develop allergic symptoms when treated with CS-derived medical products.

CS-Me were produced from highly purified CS with a degree of acetylation of 5% (Altakitin SA, Lisbon, Portugal) as previously described [8]. Briefly, CS was dissolved in 0.75% acetic acid to obtain a 1.5% solution, filtered, and poured into Petri dishes, followed by drying at room temperature. The resulting films were treated with a solution of ammonia in methanol/water, followed by intense washing with distilled water, and drying. Finally, the films were cut into the required size and sterilised by ethylene oxide.

CS nerve guides were manufactured by Medovent GmbH (Mainz, Germany) under ISO 13485 conditions from chitin tubes made following three main procedures: the extrusion process, distinctive washing, and hydrolysis steps to reach the required medium degree of acetylation (DAII). Tubes were finally cut into lengths of 12 mm and treated with ethylene oxide for sterilisation.

Analysis of the Regenerative Potential of CS-Me on Cultures of Autonomic ganglia

Autonomic Ganglia Dissection

For this study, adult male Wistar rats (Envigo, Udine, Italy) weighing 190–220 g were used. All procedures were performed in accordance with the Ethics Committee and the European Communities Council Directive of 24 November 1986 (86/609/EEC). Adequate measures were taken to minimise pain and discomfort taking into account human endpoints for animal suffering and distress.

The rats were humanely killed by lethal injection of anaesthetic solution with tiletamine + zolazepam (Zoletil®; Virbac, Carros, France) i.m. (3 mg/kg).

Rats were placed under a surgical microscope with the ventral side facing up and the caudal end oriented toward the dissector. Using forceps the neck skin and muscles were removed allowing access to the carotid artery that runs alongside the trachea. The carotid bifurcation, at the C2–C3 level, represents an important landmark to identify the superior cervical ganglia that appears as an almond-shaped structure surrounded by a connective tissue capsule closely attached to the artery. Once the ganglion was identified, using fine forceps it was dissected. Following the sympathetic trunk along the thoracic level it was possible to identify the stellate or cervicothoracic ganglion, a large ganglion probably formed by the fusion of the lower two cervical and the first thoracic ganglia. Dissection of these ganglia induced acute axotomy of the autonomic neuronal somata located within the ganglia because the pre- and postganglionic fibres had been transected. Culturing of primary organotypic explants thereby represents an *ex vivo* model of acutely axotomised neurones for studying neurite outgrowth and axonal regeneration processes [9].

Autonomic Ganglia Explant Cultures

The experiments were performed using organotypic cultures of the superior cervical and stellate (cervicothoracic) ganglia harvested as a model for surgical transection of postganglionic sympathetic nerves during RP.

The autonomic explants containing acutely axotomised autonomic neurones were cultured on two different substrates: CS-Me and glass coverslips (control).

After harvesting, the connective tissue capsule around the ganglia was removed and each ganglion was cut in half to aid the attachment on the CS-Me, a 50 μ L drop of Geltrex Matrigel (Thermo Fisher Scientific, Waltham, MA, USA) in F12 medium (50% v/v) was applied on the substrate before seeding the explants. After 2 h incubation at 37 °C, serum-free [10] culture medium with nerve growth factor (50 ng/mL; Invitrogen, Karlsruhe, Germany) was slowly added to the plate.

Immunofluorescence

After 3 days of culture, autonomic explants were fixed in 4% paraformaldehyde (SIC, Società Italiana Chimici, Rome, Italy) for 15 min, washed in 0.1 M phosphate buffer (pH 7.2) and processed for immunofluorescence analysis.

Samples were permeabilised, blocked (0.1% Triton X-100, 10% normal goat serum/0.1% NaN₃, 1 h) and incubated over-night in anti- β III-Tubulin (mouse, monoclonal, 1:1000; Sigma-Aldrich, St. Louis, MO, USA) primary antibody; after incubation with secondary antibody goat anti-mouse IgG Alexa-Fluor-488-conjugated (1:200; Molecular Probes, Eugene, OR, USA) for 1 h, autonomic explants were mounted with a Dako fluorescent mounting medium (Dako, Glostrup, Denmark).

Quantification of Neurite Outgrowth

Autonomic ganglia were scanned using a Zeiss LSM800 confocal laser microscopy system (Zeiss, Jena, Germany). For each sample, confocal Z-stacks were used and different images ($\times 10$) were captured in order to reconstruct the entire ganglia.

To evaluate the regenerative capability of the autonomic ganglia on the CS-Me, Neurite J (ImageJ plugin) was used and two different parameters were evaluated: neurite extension and axonal sprouting [11].

Evaluation of CS Effect on the Proliferation of Different Cancer Cell Lines

In vitro Cell Tests On CS-based Membranes

In vitro cell tests were performed using LN-Cap, DU-145 and PC3 cell lines. The cytotoxicity test was carried out with the

dissolution products of CS-Me, whilst LN-Cap, DU-145 and PC3 adhesion, proliferation and protein expression were evaluated on a CS coating, as detailed below.

Dissolution Products of CS-Me

The effect of the CS-Me-based material extracts was studied on LN-Cap, DU-145 and PC3 cell lines. Material extracts were prepared by incubating CS-Me in Dulbecco's Modified Eagle Medium-F12 (DMEM-F12; Sigma-Aldrich) supplemented with 100 U/mL penicillin, 0.1 mg/mL streptomycin, 1 mM sodium pyruvate, 4 mM L-glutamine (all Sigma-Aldrich), and stored at 37 °C in a humidified atmosphere of 5% CO₂ for 13 days. As control media, samples of culture medium without CS were maintained in the same conditions as the CS-Me samples and then collected after 15 days. Then, the proliferation assay was carried out using the collected media. In detail, LN-Cap, DU-145 and PC3 cells were seeded onto Petri dishes and cultivated in the previously prepared extract media, at a density of 5×10^3 cells/cm². After 1, 3, and 6 days *in vitro*, cells were trypsinised and counted in a Burker haemocytometer chamber. Experiments were performed as technical triplicates. The counts obtained from assays were analysed, averaged, and expressed as logarithmic scale of viable cells/mm² \pm SD.

Proliferation Assay on CS Coating

Culture wells were coated with a solution of 2 mg/mL CS in 0.1% acetic acid (EMD Biosciences Inc., San Diego, CA, USA) or with 0.1% acetic acid alone. Briefly, the solutions were distributed in an excess volume into each well to ensure the entire surface area was covered. Plates were placed at 4 °C overnight. The next day, before plating the prostate cancer cells, the remaining CS or acetic acid solution was aspirated. Then the proliferation assay was carried out using LN-Cap, DU-145 and PC3 cells. Cell lines were seeded and cultivated in Roswell Park Memorial Institute (RPMI) medium supplemented with 100 U/mL penicillin, 0.1 mg/mL streptomycin, 1 mM sodium pyruvate, 4 mM L-glutamine (all Sigma-Aldrich), and 2% fetal bovine serum, at a density of 5×10^3 cells/cm² on coated Petri dishes. After 2, 5, and 7 days *in vitro*, cells were trypsinised and counted in a Burker haemocytometer chamber. Experiments were performed as technical triplicates.

In vivo Analysis of Regenerative Capability of CS-Me for Median Nerve Repair

Animal and Surgical Procedure

The functional animal study was performed with adult female Wistar rats, weighing ~200 g. All procedures were approved

by the Bioethics Committee of the University of Torino, by the Institutional Animal Care and Use Committee of the University of Torino, and by the Italian Ministry of Health, in accordance with the European Communities Council Directive European Communities Council (2010/63/EU), the National Institutes of Health guidelines, and the Italian Law for Care and Use of Experimental Animals (DL26/14).

The rats were housed at a constant temperature and humidity, under 12–12 h light/dark cycles, with free access to food and water. The rats were randomly divided into two experimental groups: (i) median nerve repaired with CS-Me (NeuroShield™, Monarch Bioimplants GmbH, Root, Switzerland) and (ii) median nerve repaired with CS nerve guide (Reaxon®, Medovent GmbH).

Once the rats were under general anaesthesia (Zoletil [Virban] + Xilazina [Bayer Corp., Whippany, NJ, USA] by intraperitoneal injection [40 + 5 mg/kg]), the region was shaved and disinfected with povidone-iodine (Betadine). All surgical procedures were performed under a high magnification surgical microscope.

A median nerve segment of 8 mm was removed from the left forelimb, the CS-Me were rolled up to obtain a 12 mm long conduit that was used to bridge the nerve defect. The nerve guide was sutured with one 9/0 epineural suture at each end (Fig. 1). In the CS-nerve-guide group, a median nerve segment was removed from the left forelimb and a 12 mm chitosan nerve guide (Medovent GmbH) was used to bridge the nerve defect. The nerve guide was sutured with one 9/0 epineural suture at each end. Both devices were immersed in sterile saline for at least 10 min before implantation. In the right forelimb a segment of 12 mm of median nerve was harvested in order to prevent interference with the functional test.

At the end of the surgical procedure the skin was sutured with a 3/0 suture. After 2, 6 and 12 weeks, the rats were killed humanely by anaesthetic overdose of Zoletil + Xilazina (>60 mg/kg and >10 mg/kg) by intraperitoneal injection, and the regenerated nerves were harvested for further analysis.

Postoperative Assessment of Functional Recovery: Grasping Test

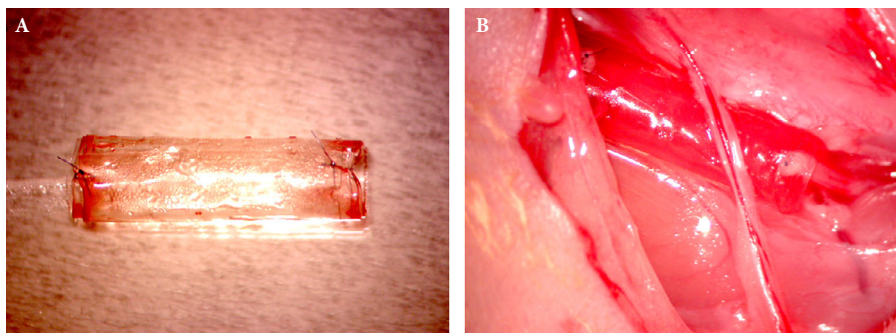
The grasping test was performed to evaluate the functional recovery after median nerve reconstruction with CS-Me and the standard CS nerve guide. The grasping test is a simple method to assess the flexor function in the rat median nerve model and was first introduced by Bertelli and Mira [12]. The grasping test combines the evaluation of the individual grasping behaviour (fine motor skills) and regained grip force (gross motor skills). This behavioural test is now widely used and commonly applied to evaluate the functional recovery of the median nerve after traumatic injury [13–20].

The grasping test for measurement of the forelimb grip force (in g) was performed in both experimental groups using a commercial testing device consisting of a triangular grid connected to a precision dynamometer (BS-GRIP Grip Meter; 2 Biological Instruments, Varese, Italy) [18]. The test is carried out by holding the rat by its tail and lowering it towards the device and then, when the rat grips the grid, pulling it upward until it loses its grip. Each rat was tested three times and the maximum weight that the rat manages to hold on before losing its grip was recorded.

Resin Embedding

At the time of euthanasia, a 10-mm-long median nerve segment was harvested immediately distal to the injury site in nerve repaired with either the CS-Me or standard CS nerve guide. A 4/0 suture was used to mark the proximal stump of the nerve segment. Samples were fixed by immediate immersion in 2.5% glutaraldehyde (SIC Società Italiana Chimici) in 0.1 M phosphate buffer (pH 7.4) for 5–6 h at 4 °C. Specimens were then post-fixed in 2% osmium tetroxide (SIC Società Italiana Chimici) for 2 h and dehydrated in passages in ethanol (Sigma-Aldrich) from 30% to 100% (5 min each passage). After two passages of 7 min in propylene oxide and overnight in a 1:1 mixture of propylene oxide (Sigma-Aldrich) and Glauerts' mixture of

Fig. 1 Representative picture of the CS-Me implantation. **(A)** CS-Me rolled up to form the nerve conduit; **(B)** Implanted conduit.



resins, samples were embedded in Glauerts' mixture of resins (made of equal parts of Araldite M and the Araldite Harter, HY 964; Sigma Aldrich). In the resin mixture, 0.5% of the plasticiser dibutylphthalate (Sigma-Aldrich) was added. For the final step, 2% of accelerator 964 was added to the resin in order to promote the polymerisation of the embedding mixture at 60 °C.

Staining and Light Microscopy

Semi-thin transverse sections of 2.5- μm thickness were cut starting from the distal stump of each median nerve specimen using an Ultracut UCT ultramicrotome (Leica Microsystems, Wetzlar, Germany) and stained with 1% toluidine blue for high-resolution light microscopic examination and design-based stereology.

Design-based Quantitative Morphology

A DM4000B microscope equipped with a DFC320 digital camera and an IM50 image manager system (Leica Microsystems) was used for stereology.

On one randomly selected toluidine blue stained semi-thin section, the total cross-sectional area of the whole nerve was measured at the light microscopic level and 12–16 sampling fields were selected using a systematic random sampling protocol. In each sampling field, a two-dimensional dissector procedure, which is based on sampling the 'tops' of fibres, was adopted in order to avoid the 'edge effect' [21,22].

For the assessment of regenerated nerves the following parameters were estimated:

- Cross-sectional area.
- Density of myelinated nerve fibres.
- Number of myelinated fibres.
- Axons diameter of myelinated fibres.
- Myelin thickness.
- Axon diameter/fibre diameter (g-ratio).

Analysis of Tissue Reaction

Animal and Surgical Procedure

The analysis of the tissue reaction was performed on the proximal halves of the regenerated tissue repaired with either CS-Me or standard CS nerve guide harvested at 2, 6 and 12 weeks after injury.

Histological Procedures

Specimens were harvested and fixed overnight at 4 °C in 4% paraformaldehyde (Sigma-Aldrich) diluted in PBS (Biochrom

GmbH, Berlin, Germany). Afterwards, the samples were stored in 70% ethanol before paraffin-embedding in a Citadel tissue embedding-automatic unit (Shandon Citadel 2000; Thermo Fisher Scientific). Series of 40 blind-coded cross-sections (thickness 7 μm) starting from mid-graft level were prepared.

Immunofluorescence

Two nerve cross-sections, consecutive to the haematoxylin and eosin stained ones, were immunohistologically stained for activated macrophages (ED1) in order to assess the degree of a possible foreign body response. Upon blocking in 5% rabbit serum (Sigma-Aldrich) diluted in PBS, sections were stained with primary mouse anti-ED1 antibody (1:1000 diluted in blocking solution; MCA275R Serotec, Oxford, UK) overnight at 4 °C, washed thrice in PBS and stained with Alexa 555-conjugated secondary goat anti-mouse antibody (1:1000 diluted in blocking solution; A21422; Invitrogen) for 1 h at room temperature. After washing in PBS again, 4',6'-diamidino-2-phenylindole (DAPI; 1:2000 diluted in PBS; Sigma Aldrich) was applied for nuclear counterstaining (2 min at room temperature), before mounting with Mowiol mounting medium (Sigma-Aldrich). Representative photomicrographs were taken at $\times 80$. In each section, 4–6 randomly selected areas in the outer area of the nerve cross-section were evaluated for the number of ED1-immunopositive signals per mm^2 using the ImageJ software version 1.48 (National Institutes of Health, Bethesda, MD, USA). DAPI staining served to clearly identify ED1-immunopositive cells.

Statistical Analysis

For *in vitro* experiments, statistical analysis was performed using one-way ANOVA and *post hoc* Bonferroni.

For neurite outgrowth assays from autonomic ganglia, statistical analysis was performed using the two-sample *t*-test. Statistical analysis was performed using the Statistical Package for the Social Sciences (SPSS®), version (SPSS statistics v20, IBM Corp., Armonk, NY, USA).

The level of significance was set at $*P \leq 0.05$, $**P \leq 0.01$, and $***P \leq 0.001$. Values were expressed as mean \pm standard deviation (SD).

For *in vivo* assessment of regenerated nerve morphometry, statistical analysis was performed again using SPSS software. Statistical analysis was performed using the two-sample *t*-test. The level of significance was set at $*P \leq 0.05$, $**P \leq 0.01$, and $***P \leq 0.001$. Values are expressed as mean \pm standard deviation (SD).

Results

CS-Me Represents a Permissive Substrate for Neurite Regeneration and Axonal Elongation of Autonomic Explant Ganglia

To evaluate the pro-regenerative capability of CS-Me, we cultured autonomic explant ganglia over 3 days and determined the numbers of extending neurites at certain distance from the explant body according to the Sholl method [11].

Overall neuritic sprouting was much enhanced in the control condition and CS-Me explants (Fig. 2). As shown in the graphs (Fig. 3), autonomic explant ganglia cultured on CS-Me had a longer neuritic length compared to the control condition.

Morphological analysis of explanted ganglia stained with β III-tubulin showed a high neuritic outgrowth and strong neurite arborisation supporting the pro-regenerative effect of CS-Me (Fig. 2).

Dissolution Products of CS-Me Negatively Affect Proliferation of LN-Cap, DU-145 and PC3 Cell Lines

The proliferation of three different human prostate cancer cell lines: DU-145, LN-Cap and PC3 cultured in medium containing dissolution products of CS-Me were evaluated. After 15 days of CS film dissolution at 37 °C, media collected were used to cultivate three cell lines and proliferation assays were carried out. Cells were plated and cultured in the presence of conditioned media and their proliferation was evaluated after 1, 3 and 6 days. As control media, samples of culture medium without dissolution products of CS-Me maintained in the same conditions were collected after 15 days. The proliferation assay was performed after 1, 3 and 6 days on DU-145, LN-Cap and PC3 cells cultured with this control condition medium.

The results demonstrate that cancer cells grown in conditioned medium with the dissolution products from the CS-Me had a significantly ($P < 0.05$) lower proliferation rate as compared to cells grown in control medium (Fig. 4).

Fig. 2 Morphology. Axonal outgrowth of organotypic autonomic ganglia cultured, stained with anti- β III-tubulin, on CS-Me (**B–D**) and control (ctr) substrate represented by glass slides (**A–C**).

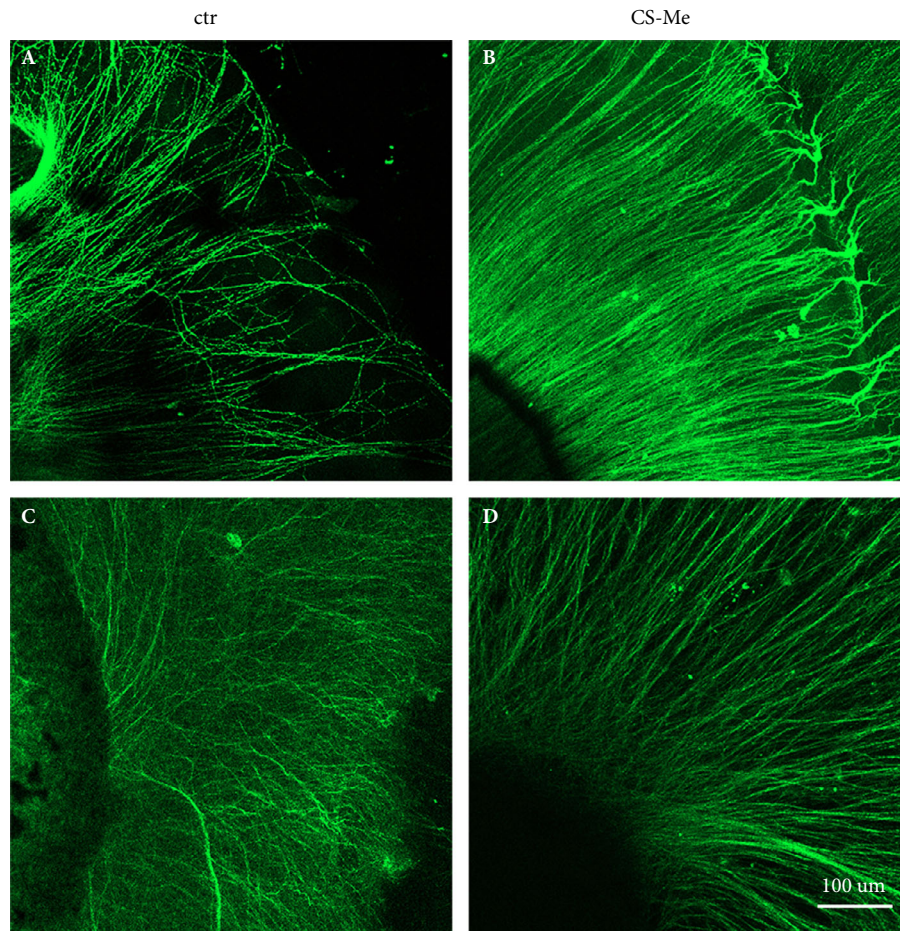


Fig. 3 Quantification of sprouting and neurite elongation. Bar graph and line graph depicting quantification of organotypic autonomic ganglia cultured on CS-Me (red) and the control (CTR) condition (blue).

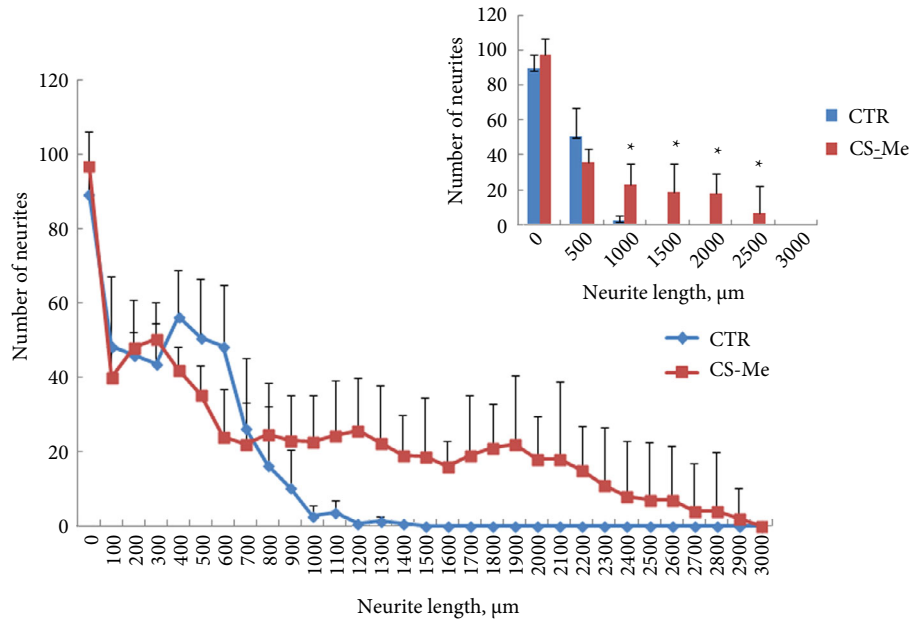
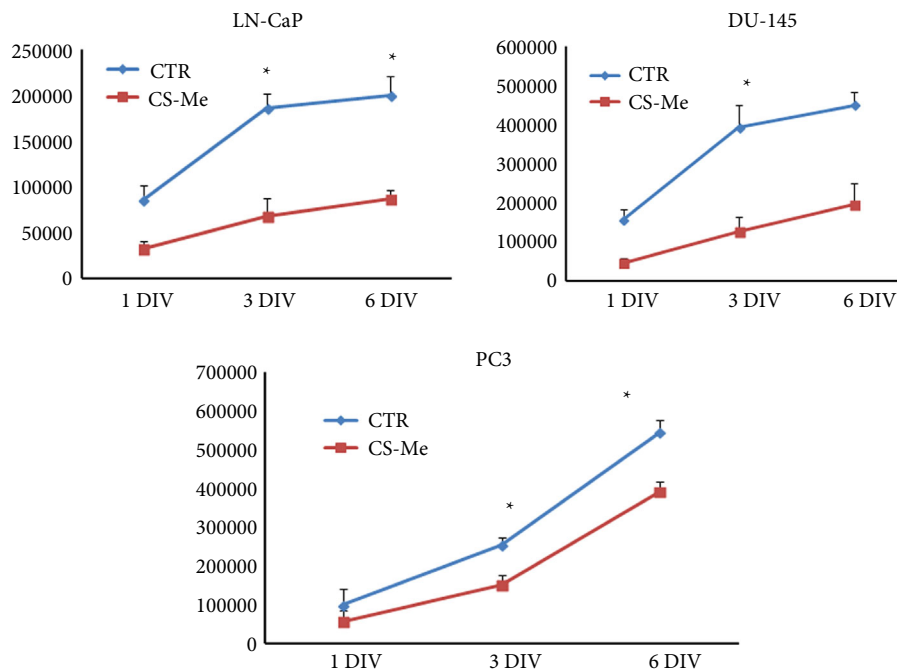


Fig. 4 Effects of dissolution products of CS-Me. Line graph depicting the proliferation of different human prostate cancer cell lines: LN CaP, DU-145 and PC3 cultured in medium collected after 15 days of CS film dissolution. * $P < 0.05$. CTR, control.

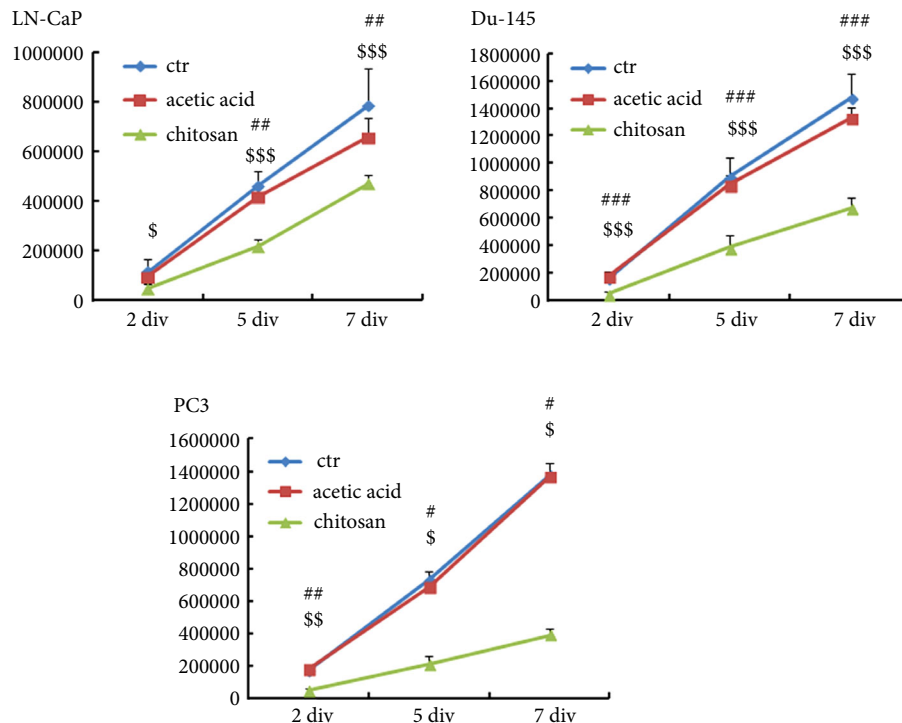


Direct Contact of Human Prostate Cancer Cell Lines with CS Coating Substantially Alter their Morphology and Proliferation Rate

The anti-proliferative effect of CS was further tested on three different human prostate cancer cell lines: DU-145,

LN-Cap and PC3. Cells were plated in three different experimental conditions: no-coating (control), CS coating, and acetic acid coating (the latter represents a control of the toxicity, as it is the substance in which CS is dissolved in), and the proliferation assay was performed after 2, 5 and 7 days.

Fig. 5 Effects of cell direct contact with CS coating. Proliferation curve experiment: LN-CaP, Du-145 and PC3 cell lines were cultivated on the control (ctr), on 0.1% acetic acid coating, and on CS coating. Results showed significantly lower proliferation of cell lines cultured on CS. $^{\$/\#\#\#}P < 0.05$; $^{\$/\#\#\#}P \leq 0.01$; $^{\$/\#\#\#}P \leq 0.001$. $^{\$/\#\#\#}$ ctr vs CS-coating treatment; $^{\#\#\#}$ acetic acid-coating vs CS-coating treatment.



All cell lines tested showed a significant reduction in their proliferation when grown on the CS substrate. No interference with proliferation was found by cultivating the cells in the presence of a coating of acetic acid at 0.1% (Fig. 5). Cell morphology reflects the results of the proliferation experiments. Cells cultured on the CS substrate lost their normal morphology and adhesion capacity; they appeared rounded and formed clusters (Fig. 6).

CS-Me Allows Nerve Fibre Regeneration 12 weeks after Median Nerve Damage and is biologically inert

Evaluation of Functional Recovery

Functional recovery was evaluated at the 12-week time-point in regenerated median nerves repaired with CS-Me or with standard CS nerve guides by means of the grasping test for measurement of the left forelimb grip force (Fig. 7).

No significant differences in the grip forces were found between the two experimental groups at 12 weeks. It can be concluded that the CS-Me nerve conduit allowed peripheral nerve regeneration similar to the CS tube.

Interestingly, values were already close to those of healthy, uninjured limbs, which are in the range of 300 [17] to 450 g

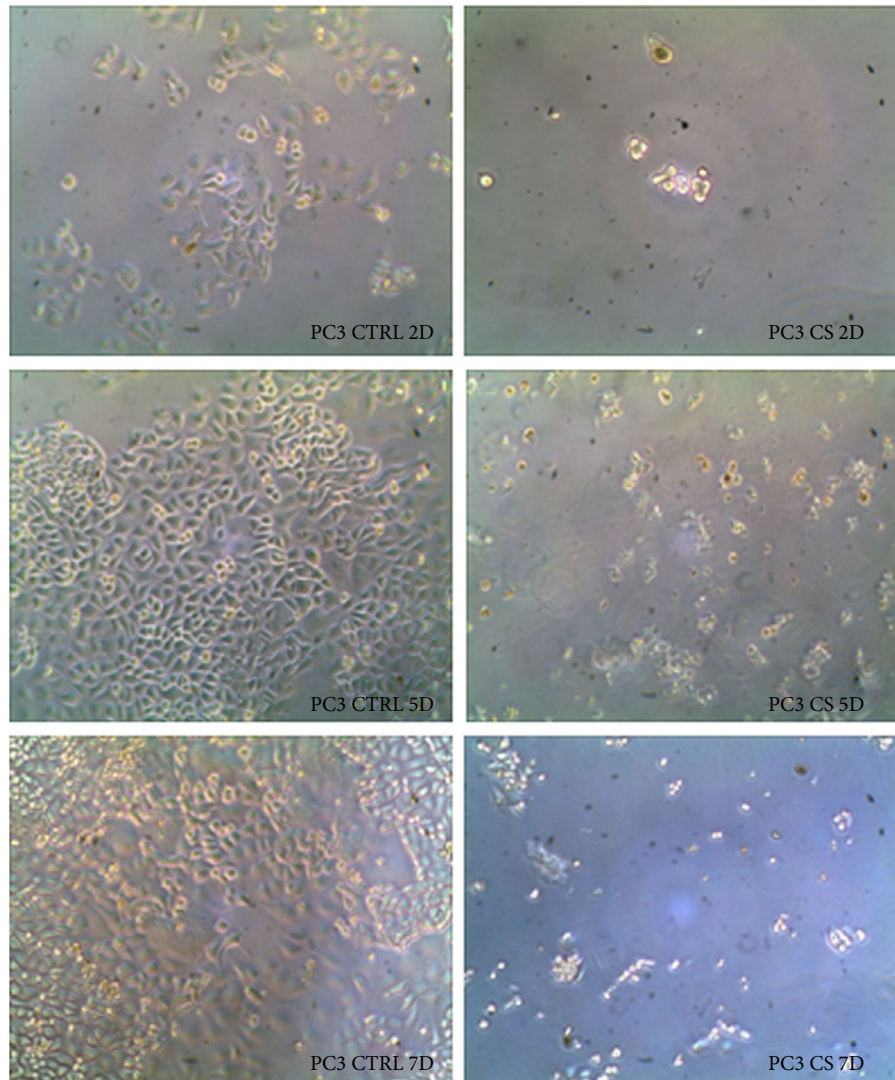
[18]. Thus, recovery is fast, also compared to results described for a direct suturing model of the rat median nerve (which is less traumatic than the gap model of this study), resulting in grip forces of merely 100 g at 12 weeks after implantation [17].

Design-based Quantitative Morphology of Myelinated Nerve Fibres

Morphological evaluation of toluidine-blue stained cross-sections of the distal part of the regenerating nerves showed the presence of myelinated regenerated nerve fibres from the two experimental groups organised in microfascicles with well-defined axoplasm and well-organised myelin sheaths (Fig. 8). Quantitative analysis (Fig. 9) showed that the cross-sectional area of the distal part of the regenerated nerves was not statistically different between the two experimental groups (Fig. 9A). Moreover, the density (Fig. 9B) and the total number of myelinated fibres (Fig. 9C) were not statistically different between the two groups.

With respect to parameters related to the nerve fibre size, axon size, myelin thickness (Fig. 9D), and g-ratio (axon diameter/fibre diameter; Fig. 9E), there were no detectable significant differences between the two groups.

Fig. 6 Effects of cell direct contact with CS coating. Morphology: representative panel depicting PC3 cell lines cultivated on the control (CTRL) and on the CS coating. Cultured cells on the CS substrate lose their normal morphology and adhesion capacity; they appear rounded and form clusters. 2D, culture at 2 days; 5D, culture at 5 days; 7D, culture at 7 days.



Evaluation of Tissue Reaction at the Implantation Site

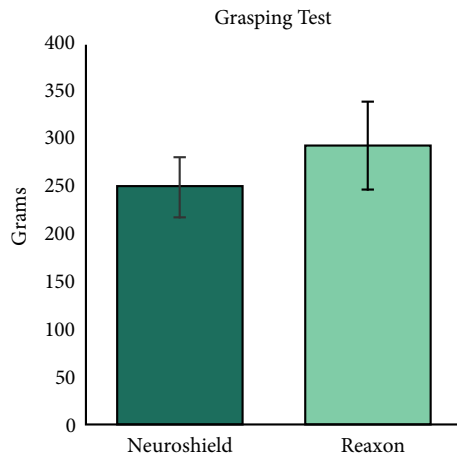
As shown in Fig. 10, ED1-immunopositive cells were detectable in all samples analysed. The bar graph in Fig. 11 shows the results from the quantification of ED1-immunopositive cells within the outer layer of the regenerated nerve tissue at mid-graft level. A significant decrease in the number of activated macrophages was detectable from 2 to 6 weeks after implantation in both, the CS-Me and CS-nerve-guide groups ($*P < 0.05$). Within the CS-nerve-guide-tube group a significant decrease in ED1-positive cells further occurred between each of the time points ($*P < 0.05$). Within the CS-Me group, both at 6 weeks and 12 weeks, the number of ED1-immunopositive cells was significantly reduced ($*P < 0.05$) in

comparison to 2 weeks after the implantation. The number of activated ED1-immunopositive macrophages was significantly lower in CS-Me samples at 6 weeks than in control samples. From 6 to 12 weeks the number of ED1-immunopositive cells further decreased in the CS-Me group but not in a significant amount anymore. The investigated materials can therefore be considered biologically inert. From these results, it can further be concluded that the tissue reaction towards the implanted material is attenuated sooner in the CS-Me group than in the standard CS-nerve-guide group.

Discussion

CS is a derivative of chitin, obtained from the exoskeleton of crustaceans, which has been receiving significant interest both

Fig. 7 *In vivo* functional analysis. Bar graph reporting the post-traumatic functional recovery assessed by the grasping test. Values for the left forelimb grip force are reported as mean \pm sd. Neuroshield, CS-Me; Reaxon, CS nerve guide.



in basic research and in clinical settings. Its chemical structure [polysaccharide composed of D-glucosamine and N-acetyl-D-glucosamine linked with $\beta(1-4)$ bond] gives it remarkable hypoallergenicity, making it an excellent candidate for the development of innovative applications in the field of medicine and surgery, also thanks to its biocompatibility, bioavailability, and lack of toxicity. For these reasons, the potential clinical applications of CS range from orthopaedics

and drug-delivery systems to scaffolds for regeneration of nerve, skin, bone, and cartilage [6,23–27].

The aims of the present study were focused on: (i) addressing the axonal-regenerative potential of CS-Me for acutely axotomised autonomic ganglion neurones in *ex vivo* cultures by modelling fibre outgrowth of the transected NVB after RP; (ii) excluding the possibility that this specific pro-regenerative biomaterial could increase the cell proliferation in a tumour site by culturing prostate cancer cell lines on CS and in presence of CS-Me dissolution products; (iii) evaluating the regenerative potential and the functional recovery of the CS-Me to repair a somatic nerve lesion; (iv) assessing the reaction of the regenerating and the surrounding tissue towards the material. For addressing study aims (iii) and (iv), we chose the rat median nerve model, which is well standardised and known to be able to elucidate nerve reconstruction conditions and to assess the regeneration process. To the best of our knowledge, to date no specific and standardised pre-clinical model exists for simulating transection of the periprostatic NVB. Furthermore, our group has profound knowledge of the rat median nerve injury and repair model and has tested varying biomaterial-based approaches for nerve repair, including CS-based nerve guides [28,29]. In addition, clinical data available to date for the application of CS-Me after RP [5] do not indicate that low biocompatibility of the material could negatively interfere with healing process. Therefore, the rat median nerve model appeared as the most appropriate model to us for

Fig. 8 Representative low- and high-magnification light photomicrographs. Toluidine blue-stained semi-thin cross-sections of nerve repaired with CS nerve guide (**A** and **B**) and CS-Me (**C** and **D**) obtained at the distal level. Scale bar, 20 μ m.

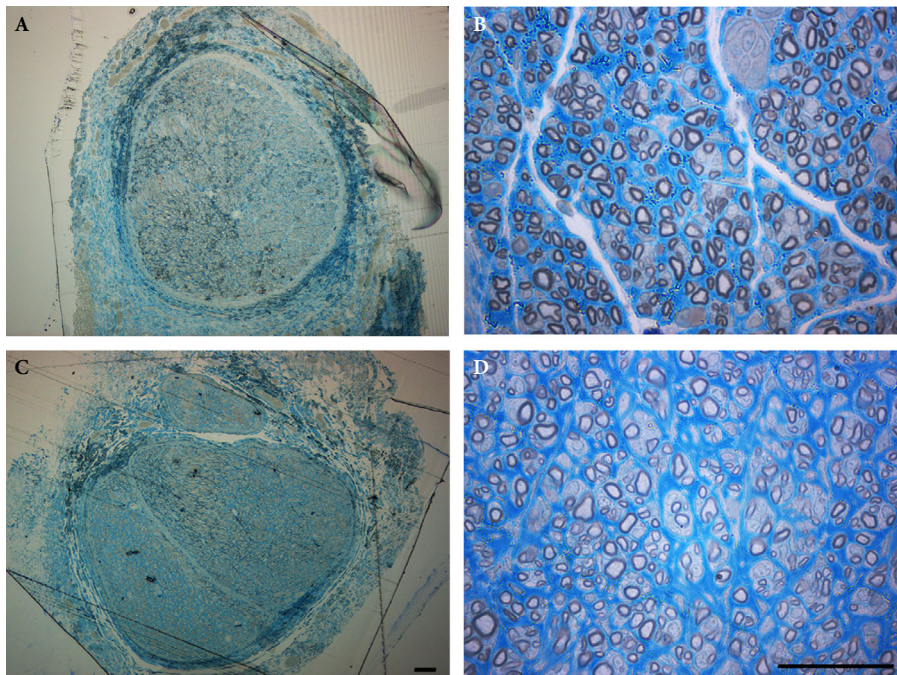
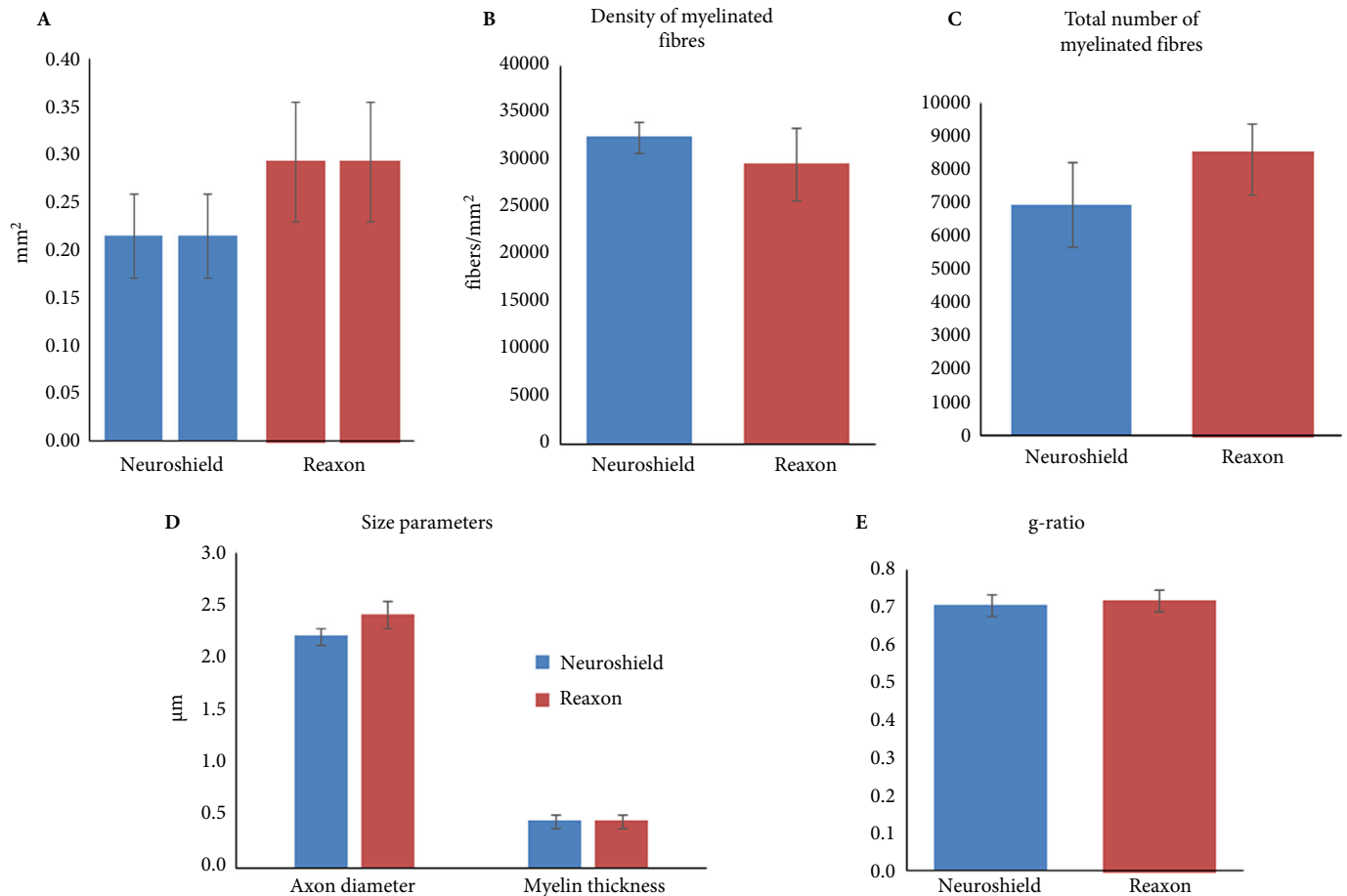


Fig. 9 Stereological assessment of regenerated nerve fibres. Stereological assessment of regenerated nerve fibres. **(A)** Nerve cross-sectional area; **(B)** density of myelinated fibres; **(C)** total number of myelinated nerve fibres; **(D)** size parameters: axon diameter, myelin thickness; **(E)** g-ratio. Data are expressed as mean \pm sd. Neuroshield, CS-Me; Reaxon, CS nerve guide.



comprehensively analyse the properties of CS-Me in nerve repair.

As regards the first study aim, we used primary organotypic cultures, which provided a multicellular *ex vivo* model that preserves both the cytoarchitecture of the tissue and the interactions amongst cells, providing a closer approximation to *in vivo* conditions [9,30]. As the prostatic plexus is innervated by autonomic nerve fibres, the regenerative potential of CS-Me was assessed through acutely axotomised organotypic sympathetic ganglion cultures that represent an innovative and original experimental model for testing autonomic nervous system regenerative properties.

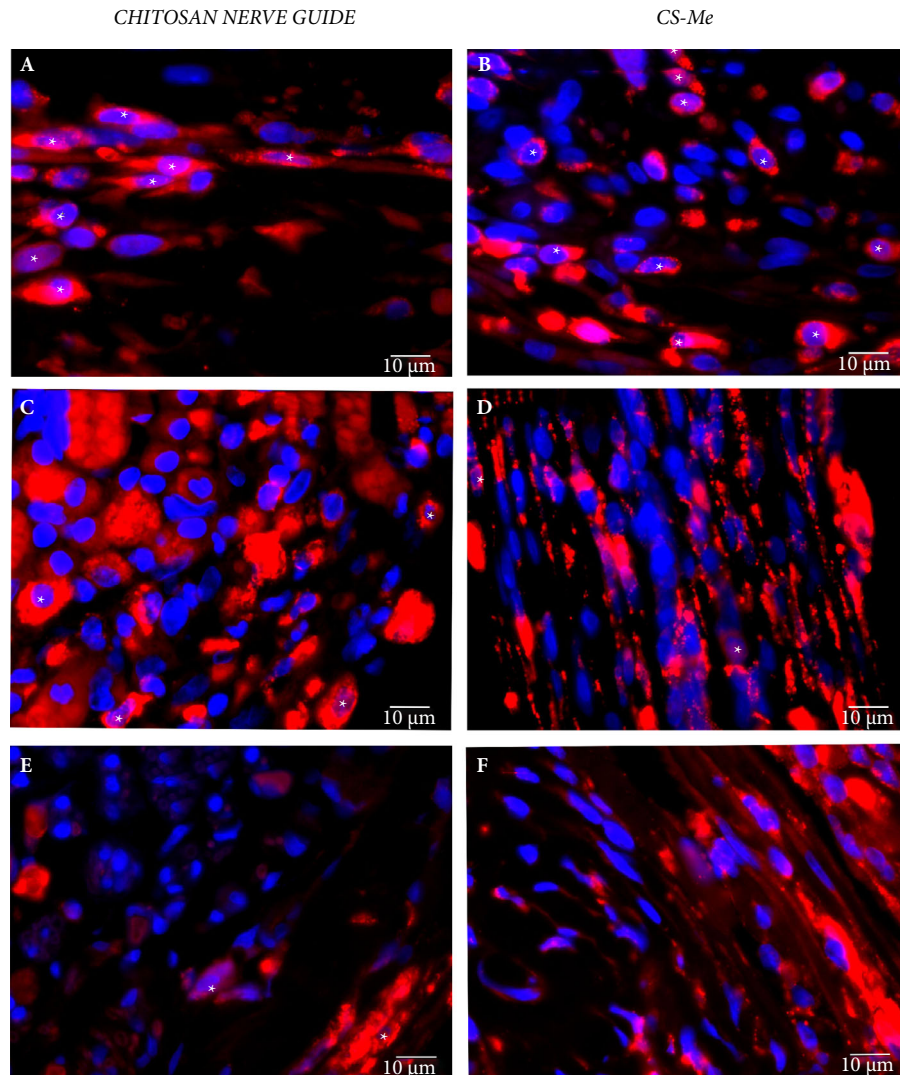
We demonstrated, for the first time in the literature, that CS-Me not only exert a pro-regenerative effect on somatic neuronal ganglia [8,27], but also on autonomic neuronal ganglia. This observation is important as it provides a possible mechanistic explanation for the positive effects of CS-Me application on functional recovery after RP [5], namely that the faster recovery of potency is due to the post-

surgical stimulation of axonal regrowth in the periprostatic NVBs.

The second aim of the present study was to analyse the safety of the use of CS-Me in surgical oncology of prostate cancer. Given the intrinsic cell supportive capacity of CS, we wanted to rule out that CS might have any negative side-effect due to a proliferative stimulation of prostate cancer cells. Alongside the pro-regenerative effects, of great interest is the anti-proliferative activity of CS reported on different tumour cell lines. Indeed, the anticancer activity of CS was proved in human breast cancer cell lines [31], in a human gastric carcinoma cell line MGC803, and in a human monocytic leukaemia cell line [32,33]. Gibot et al. [34] analysed the mechanisms underlying the anti-proliferative effect of CS on human melanoma cell lines and suggested a cell-line dependent effect on apoptosis and further proposed this type of analysis as a future instrument for assessing cancer therapies in the field of melanoma.

We wanted to test the effect of CS-Me dissolution products on the proliferation of tumour cells derived from prostate

Fig. 10 Representative photomicrographs taken from median nerve cross-sections at mid-graft level. ED1-immunopositive cells display a red cytoplasm and blue nuclei counterstained with DAPI in CS nerve guide and CS-Me. (**A-C-E**) nerve repaired with CS nerve guide harvested at 2, 6 and 12 weeks, respectively after surgery; (**B-D-F**) nerve repaired with CS-Me harvested at 2, 6 and 12 weeks, respectively after surgery. Scale bars, 10 μm . Asterisks indicate cellular profiles counted as activated ED1-immunopositive macrophages.



adenocarcinomas: lymph node, brain and bone metastasis, respectively, LN-Cap, DU-145 and PC3 cells [35,36].

It is known from the literature that CS products are able to stimulate regeneration and therefore the positive effect on the neuronal population is not only due to direct contact with the material but also from its degradation [37]. Interestingly, we observed that cancer cells grown in conditioned medium with the dissolution products from CS-Me exhibit a significantly lower proliferation rate compared to cells grown in control medium.

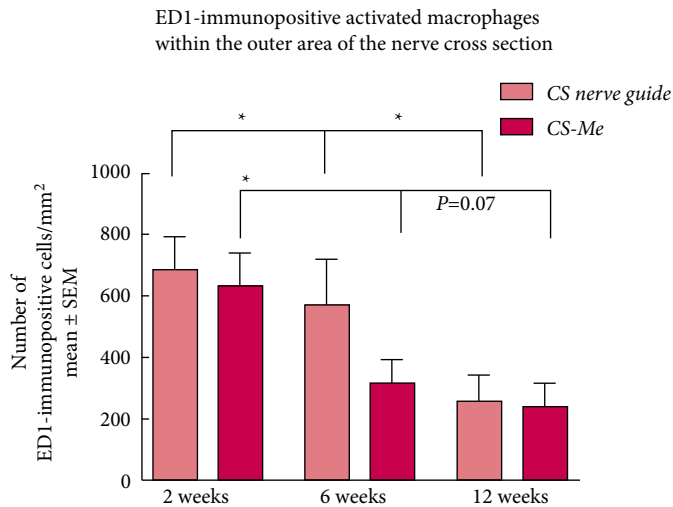
The direct contact of CS with cancer cell lines was tested with regard to cell proliferation and morphology. This experiment revealed a significant reduction in proliferation of the prostate cancer cell lines grown on the CS substrate. The analysis of the

cell morphology also reflected this aspect: cultured cells on the CS substrate lost their normal morphology and adhesion capacity, and finally appeared rounded and formed clusters.

As already explained above, for evaluating the regeneration of the damaged NVB after nerve-sparing RP with regard to functional and quantitative parameters, standardised pre-clinical models are controversial. Therefore, these additionally important aspects have been investigated in an alternative experimental model, which allows a precise, effective, and highly standardised evaluation of the same, the resection and repair of the median nerve.

In this context, the third aim of the present study was the evaluation of the CS-Me in terms of regeneration after median

Fig. 11 Quantification of ED1-immunopositive cellular profiles at regenerated median nerve mid-graft level. Bar graph depicting the mean \pm SEM number of ED1-immunopositive cells/mm² in the outer area of the analysed two nerve cross-sections per sample.



nerve transection and the assessment of functional recovery in comparison with the standard CS nerve guide that evidently represents a pro-regenerative device [25,27,28,38].

The comparison between CS-Me and the CS nerve guide revealed a substantial equivalence of the two medical devices for repairing a 10 mm-long nerve gap in the rat median nerve.

Functional recovery of neuromuscular function is the most relevant issue in a pre-clinical perspective. Behavioural testing of the recovery of the grasping function (controlled by the median nerve innervation of flexor digitorum muscles) showed no significant differences between the two devices at 12 weeks postoperatively. This result is noteworthy, as the flexion of the fingers for grasping an object is a voluntary movement, the recovery of which reflects not only the re-innervation of the muscles but also the recovery of the central control of the relevant neural pathways.

Equivalent results with these two devices were also found when comparing the quality of nerve fibre regeneration by quantitative morphological analysis (using unbiased stereology), namely no differences were found between the two experimental groups for the number, density and size of regenerated axons, as well as the myelin sheath thickness and g-ratio.

The tissue reaction towards the implanted biomaterial, addressed in the fourth aim of the present study, was similar for both devices, characterised by the absence of polymorphonuclear cells, lymphocytes, plasma cells, necrosis and fibrosis of the tissue peripheral nerve. The decreasing number of activated macrophages over time are indicators of a very mild tissue response that decreases over time. Remarkably, there were statistically significant fewer ED1-immunopositive

cells detected at 6 weeks after implantation with CS-Me in comparison to the CS nerve guide. This indicates that the CS-Me induced a milder tissue reaction at this time point, whilst at 12 weeks no differences were found between the two devices. Furthermore, there were no statistical differences in the number of ED1-immunopositive cells in CS-Me at 6 and 12 weeks, indicating steady state conditions.

Prostate cancer, whose surgical therapy, RP, remains the 'gold standard' therapy today, is increasing in incidence every year, exceeding the number of lung cancer and colorectal cancers. Following the removal of the prostate, the NVBs may be damaged, leading to functional deficits such as erectile dysfunction and incontinence. There has been much clinical research effort to minimise side-effects and limit residual functional deficiencies. Recently, Porpiglia et al. [5] reported the preliminary results of a clinical trial in which they tested CS, already known for its effectiveness in promoting nerve regeneration [8], in the form of membranes they aimed to protect the NVB following RP. They showed the feasibility of the application of CS-Me and the safety of the material, meanwhile observing a promising effect on the recovery of potency in the patients.

Taken together, the results of the present study provide strong evidence, using pre-clinical basic science models, underscoring the previously reported promising clinical results. The present results further support the view that application of CS-Me can be a simple, safe and an effective adjunct strategy to support timely functional recovery of the periprostatic plexus after nerve-sparing RP. We conclude that this approach deserves further efforts towards widespread clinical application.

Acknowledgements

We thank Monarch Bioimplants for supplying CS-Me for the study of autonomic neurones regeneration and for the dissolution products study on prostate cancer cell lines and Medovent GmbH for supplying Reaxon tubes. We thank Silke Fischer and Natascha Heidrich (Hannover Medical School) for excellent technical assistance.

Conflicts of Interest

Stefano Geuna and Francesco Porpiglia are scientific consultants for Monarch Bioimplants.

References

- Boyle P, Ferlay J. Mortality and survival in breast and colorectal cancer. *Nat Clin Pract Oncol* 2005; 2: 424–5
- Jemal A, Siegel R, Ward E et al. Cancer statistics, 2008. *CA Cancer J Clin* 2008; 58: 71–96
- Porpiglia F, Fiori C, Bertolo R et al. Five-year outcomes for a prospective randomised controlled trial comparing laparoscopic and robot-assisted radical prostatectomy. *Eur Urol Focus* 2018; 4: 80–6
- Patel VR, Samavedi S, Bates AS et al. Dehydrated human amnion/chorion membrane allograft nerve wrap around the prostatic neurovascular bundle accelerates early return to continence and potency

- following robot-assisted radical prostatectomy: propensity score-matched analysis. *Eur Urol* 2015; 67: 977–80
- 5 Porpiglia F, Bertolo R, Fiori C, Manfredi M, De Cillis S, Geuna S. Chitosan membranes applied on the prostatic neurovascular bundles after nerve-sparing robot-assisted radical prostatectomy: a phase II study. *BJU Int* 2017; 121: 472–8
 - 6 Fregnan F, Ciglieri E, Tos P et al. Chitosan crosslinked flat scaffolds for peripheral nerve regeneration. *Biomed Mater* 2016; 11: 045010. <https://doi.org/10.1088/1748-6041/11/4/045010>
 - 7 Dietzmeyer N, Förthmann M, Leonhard J et al. Two-chambered chitosan nerve guides with increased bendability support recovery of skilled forelimb reaching similar to autologous nerve grafts in the rat 10 mm median nerve injury and repair model. *Front Cell Neurosci* 2019; 13: 149
 - 8 Wrobel S, Serra SC, Ribeiro-Samy S et al. *In vitro* evaluation of cell-seeded chitosan films for peripheral nerve tissue engineering. *Tissue Eng Part A* 2014; 20: 2339–49
 - 9 Geuna S, Raimondo S, Fregnan F, Haastert-Talini K, Grothe C. *In vitro* models for peripheral nerve regeneration. *Eur J Neurosci* 2016; 43: 287–96
 - 10 Fueshko S, Wray S. LHRH cells migrate on peripherin fibers in embryonic olfactory explant cultures: an *in vitro* model for neurophilic neuronal migration. *Dev Biol* 1994; 166: 331–48
 - 11 Torres-Espín A, Santos D, González-Pérez F, del Valle J, Navarro X. Neurite-J: an image-J plug-in for axonal growth analysis in organotypic cultures. *J Neurosci Methods* 2014; 236: 26–39
 - 12 Bertelli JA, Mira JC. The grasping test: a simple behavioral method for objective quantitative assessment of peripheral nerve regeneration in the rat. *J Neurosci Methods* 1995; 58: 151–5
 - 13 Casal D, Mota-Silva E, Iria I et al. Reconstruction of a 10-mm-long median nerve gap in an ischemic environment using autologous conduits with different patterns of blood supply: a comparative study in the rat. *PLoS One* 2018; 13: e0195692. <https://doi.org/10.1371/journal.pone.0195692>
 - 14 Ghizoni MF, Bertelli JA, Grala CG, da Silva RM. The anabolic steroid nandrolone enhances motor and sensory functional recovery in rat median nerve repair with long interpositional nerve grafts. *Neurorehabil Neural Repair* 2013; 27: 269–76
 - 15 Ho CY, Yao CH, Chen WC, Shen WC, Bau DT. Electroacupuncture and acupuncture promote the rat's transected median nerve regeneration. *Evid Based Complement Alternat Med* 2013; 2013: 514610
 - 16 Moges H, Wu X, McCoy J et al. Effect of 810 nm light on nerve regeneration after autograft repair of severely injured rat median nerve. *Lasers Surg Med* 2011; 43: 901–6
 - 17 Papalia I, Tos P, Stagno d'Alcontres F, Battiston B, Geuna S. On the use of the grasping test in the rat median nerve model: a re-appraisal of its efficacy for quantitative assessment of motor function recovery. *J Neurosci Methods* 2003; 127: 43–7
 - 18 Ronchi G, Nicolino S, Raimondo S et al. Functional and morphological assessment of a standardized crush injury of the rat median nerve. *J Neurosci Methods* 2009; 179: 51–7
 - 19 Sinis N, Schaller HE, Schulte-Eversum C et al. Nerve regeneration across a 2-cm gap in the rat median nerve using a resorbable nerve conduit filled with Schwann cells. *J Neurosurg* 2005; 103: 1067–76
 - 20 Stossel M, Rehra L, Haastert-Talini K. Reflex-based grasping, skilled forelimb reaching, and electrodiagnostic evaluation for comprehensive analysis of functional recovery – The 7-mm rat median nerve gap repair model revisited. *Brain Behav* 2017; 7: e00813
 - 21 Geuna S. Appreciating the difference between design-based and model-based sampling strategies in quantitative morphology of the nervous system. *J Comp Neurol* 2000; 427: 333–9
 - 22 Geuna S, Tos P, Battiston B, Guglielmo R. Verification of the two-dimensional disector, a method for the unbiased estimation of density and number of myelinated nerve fibers in peripheral nerves. *Ann Anat* 2000; 182: 23–34
 - 23 Martins EA, Michelacci YM, Baccarin RY, Cogliati B, Silva LC. Evaluation of chitosan-GP hydrogel biocompatibility in osteochondral defects: an experimental approach. *BMC Vet Res* 2014; 10: 197. <https://doi.org/10.1186/s12917-014-0197-4>
 - 24 Xu B, Jiang G, Yu W et al. Preparation of poly(lactic-co-glycolic acid) and chitosan composite nanocarriers via electrostatic self assembly for oral delivery of insulin. *Mater Sci Eng C Mater Biol Appl* 2017; 78: 420–8
 - 25 Haastert-Talini K, Geuna S, Dahlin LB et al. Chitosan tubes of varying degrees of acetylation for bridging peripheral nerve defects. *Biomaterials* 2013; 34: 9886–904
 - 26 Brown MA, Daya MR, Worley JA. Experience with chitosan dressings in a civilian EMS system. *J Emerg Med* 2009; 37: 1–7
 - 27 Meyer C, Stenberg L, Gonzalez-Perez F et al. Chitosan-film enhanced chitosan nerve guides for long-distance regeneration of peripheral nerves. *Biomaterials* 2016; 76: 33–51
 - 28 Ronchi G, Fornasari BE, Crosio A et al. Chitosan tubes enriched with fresh skeletal muscle fibers for primary nerve repair. *Biomed Res Int* 2018; 2018: 9175248. <https://doi.org/10.1155/2018/9175248>
 - 29 Crosio A, Fornasari BE, Gambarotta G et al. Chitosan tubes enriched with fresh skeletal muscle fibers for delayed repair of peripheral nerve defects. *Neural Regen Res* 2019; 14: 1079–84
 - 30 Morano M, Wrobel S, Fregnan F et al. Nanotechnology versus stem cell engineering: *in vitro* comparison of neurite inductive potentials. *Int J Nanomed* 2014; 9: 5289–306
 - 31 Jiang M, Ouyang H, Ruan P et al. Chitosan derivatives inhibit cell proliferation and induce apoptosis in breast cancer cells. *Anticancer Res* 2011; 31: 1321–8
 - 32 Qi LF, Xu ZR, Li Y, Jiang X, Han XY. *In vitro* effects of chitosan nanoparticles on proliferation of human gastric carcinoma cell line MGC803 cells. *World J Gastroenterol* 2005; 11: 5136–41
 - 33 Salah R, Michaud P, Mati F et al. Anticancer activity of chemically prepared shrimp low molecular weight chitin evaluation with the human monocyte leukaemia cell line, THP-1. *Int J Biol Macromol* 2013; 52: 333–9
 - 34 Gibot L, Chabaud S, Bouhout S, Bolduc S, Auger FA, Moulin VJ. Anticancer properties of chitosan on human melanoma are cell line dependent. *Int J Biol Macromol* 2015; 72: 370–9
 - 35 Gately S, Twardowski P, Stack MS et al. Human prostate carcinoma cells express enzymatic activity that converts human plasminogen to the angiogenesis inhibitor, angiostatin. *Cancer Res* 1996; 56: 4887–90
 - 36 Liao CD, Zhang F, Guo RM et al. Peripheral nerve repair: monitoring by using gadofluorine M-enhanced MR imaging with chitosan nerve conduits with cultured mesenchymal stem cells in rat model of neurotmesis. *Radiology* 2011; 262: 161–71
 - 37 Zhao Y, Wang Y, Gong J et al. Chitosan degradation products facilitate peripheral nerve regeneration by improving macrophage-constructed microenvironments. *Biomaterials* 2017; 134: 64–77
 - 38 Gonzalez-Perez F, Cobiainchi S, Geuna S et al. Tubulization with chitosan guides for the repair of long gap peripheral nerve injury in the rat. *Microsurgery* 2015; 35: 300–8

Correspondence: Francesco Porpiglia, Division of Urology, Department of Oncology, San Luigi Gonzaga Hospital, University of Turin, Regione Gonzole 10, Orbassano 10043, Italy.

e-mail: francesco.porpiglia@unito.it

Abbreviations: CS(-Me), chitosan (membrane); DAPI, 4',6'-diamidino-2-phenylindole; dHACM, dehydrated human amnion/chorion membrane; NVB, neurovascular bundle; (RA)RP, (robot-assisted) radical prostatectomy.